

NOTATION

a	= radius of resin particle, cm.
C	= equilibrium capacity of resin for carbon dioxide, meq./dry g. (as HCO_3^-)
C_{imm}	= immobilized carbon dioxide within resin particle, moles CO_2 /1,000 g. resin
C_L	= concentration of carbon dioxide in liquid, moles CO_2 /1,000 g. solution
C_R	= concentration of carbon dioxide in resin phase, moles CO_2 /1,000 g. resin
C_{R0}	= concentration of carbon dioxide in resin phase at time = 0, moles CO_2 /1,000 g. resin
$C_{R\infty}$	= concentration of carbon dioxide in resin phase at time = ∞ , moles CO_2 /1,000 g. resin
d	= distribution coefficient, defined as the ratio of carbon dioxide absorbed by the solid phase to that by the associated salt solution, dimensionless
D	= diffusion coefficient, sq.cm./min.
D'	= $D/(1 + \alpha)$
K	= equilibrium constant, defined by Equation (1)
k_G	= gas phase mass transfer coefficient, g. moles/(min.) (atm.) (sq.cm.)
k_L	= liquid phase mass transfer coefficient, cm./min.
K_L	= overall liquid phase mass transfer coefficient, cm./min.
M_t	= total amount of carbon dioxide absorbed by resin at time t , moles CO_2 /1,000 g. resin
M_∞	= total amount of carbon dioxide absorbed by resin

at time ∞ , moles CO_2 /1,000 g. resin

P_{CO_2}	= partial pressure of carbon dioxide in gas phase, atm.
R	= gas constant
r	= distance from particle center, cm.
RH	= relative humidity, fraction
s	= equilibrium solubility of carbon dioxide in solution surrounding resin beads, moles CO_2 /1,000 g. solution - atm. carbon dioxide partial pressure
t	= time, min.
Z	= thickness of gas boundary layer, cm.

Greek Letters

α	= C_{imm}/C_R
β	= $\eta/2\xi$
δ	= thickness of solution film, cm.
ξ	= $\frac{1}{2} \left(\frac{k_G}{s\delta} + \frac{k_L}{\delta} + \frac{3k_L}{ad} \right)$
∇^2	= Laplacian
η	= $3k_Gk_L/a\delta ds$

LITERATURE CITED

1. Robins, J., Ph.D. thesis, Polytechnic Institute of Brooklyn, N. Y. (1959).
2. Saber, T. M. H., Ph.D. thesis, Polytechnic Institute of Brooklyn, N. Y. (1965).
3. Katchalsky, A., and P. Spitnik, *J. Poly. Sci.*, **2**, 432 (1947).
4. Helfferich, F., "Ion Exchange," McGraw-Hill, New York (1962).
5. Crank, J., "The Mathematics of Diffusion," Oxford Univ. Press, London, England (1957).
6. Sherwood, T. K., and R. L. Pigford, "Absorption and Extraction," McGraw-Hill, New York (1952).

Manuscript received December 13, 1967; revision received January 15, 1969; paper accepted January 20, 1969.

Momentum, Heat, and Mass Transfer to a Continuous Cylindrical Surface in Axial Motion

GANAPATHY VASUDEVAN and STANLEY MIDDLEMAN

University of Rochester, Rochester, New York

The transport equations for the region exterior to a cylindrical jet issuing continuously from an orifice are solved through the introduction of a similarity transform. The possibility of mass transfer normal to the jet is allowed. Of particular interest are the local transport coefficients (c_f , N_{Nu} , N_{Sh}) and their dependence on the rate of transfer from the jet.

In two areas of technological importance, namely, fiber spinning and liquid fuel injection, it is necessary to have estimates for the transport coefficients that characterize

heat, mass, and momentum transfer between the cylindrical jet and the ambient fluid. Little attention has been given to this problem as regards fuel injection systems, primarily because these systems are designed so that the jet is unstable and rapidly transforms from a cylinder to

Stanley Middleman is at the University of Massachusetts, Amherst, Massachusetts.

a spray. Nevertheless, certain events which may critically determine the stability of a jet occur on the cylindrical surface. Experimental studies (3) have shown that the viscous drag on the coherent portion of the surface may play a significant role in jet breakup under certain conditions.

In fiber spinning from the melt, it is necessary to know cooling rates from the molten polymer to the ambient medium. In solution dry spinning, it is necessary to know the mass transfer rate of the evaporating solvent. In some studies (1) it has been assumed that the transfer coefficients are the same as (or simply related to) coefficients for a cylinder whose axis is perpendicular to a uniform air stream. This is clearly an oversimplification, and two studies have attempted to improve the situation.

Sakiadis (7) restricted his attention to the fluid dynamics of a continuous cylindrical surface issuing into a fluid. An integral boundary-layer type of approach was used, and from this work one may estimate velocity profiles, boundary-layer thicknesses, and local friction coefficients on a cylindrical surface. Griffith (4) extended the approach of Sakiadis to the problem of heat and mass transfer from a fiber issuing from a spinneret and performed some model experiments.

Both of these studies suffer from certain defects of an integral boundary-layer method. Hence, a more complete and exact analysis is offered here, based on the observa-

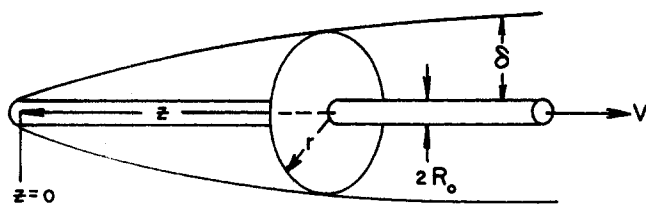


Fig. 1. Definition sketch of geometry.

tion that a similarity solution of the boundary-layer equations is possible. From the analytical solutions, it is possible to calculate local skin friction coefficients and local Nusselt and Sherwood numbers. The analysis includes the effect of high mass transfer rates, from which it is possible to calculate the reduction in drag and heat transfer due to rapid vaporization of the jet. This latter feature is of special importance for the analysis of cryogenic fuel injection.

The treatment is restricted to the laminar boundary layer on a jet of constant velocity, temperature, and concentration along the surface. While these assumptions are not valid for most fiber spinning operations, the results should nevertheless provide a framework for more exact inquiries into the dynamics of more complex systems.

THEORY

The development parallels that of a similar problem discussed in (2). Figure 1 shows the geometry of the problem. The usual boundary-layer assumptions lead to the following equations for the steady state:

$$\text{Momentum: } v_r \frac{\partial v_z}{\partial r} + v_z \frac{\partial v_z}{\partial z} = \frac{\nu}{r} \frac{\partial}{\partial r} \left(r \frac{\partial v_z}{\partial r} \right) \quad (1)$$

$$\text{Continuity: } \frac{\partial v_z}{\partial z} + \frac{1}{r} \frac{\partial (rv_r)}{\partial r} = 0 \quad (2)$$

$$\text{Heat: } v_r \frac{\partial T}{\partial r} + v_z \frac{\partial T}{\partial z} = \frac{\alpha}{r} \frac{\partial}{\partial r} \left(r \frac{\partial T}{\partial r} \right) \quad (3)$$

Chemical

$$\text{Species A: } v_r \frac{\partial x_A}{\partial r} + v_z \frac{\partial x_A}{\partial z} = \frac{D_{AB}}{r} \frac{\partial}{\partial r} \left(r \frac{\partial x_A}{\partial r} \right) \quad (4)$$

The boundary conditions appropriate to the applications mentioned above are

$$\left. \begin{aligned} v_r &= 0 \\ v_z &= 0 \end{aligned} \right\} \text{ at } r = \infty$$

$$\left. \begin{aligned} v_r &= v_{r0} \\ v_z &= V \end{aligned} \right\} \text{ at } r = R_0, z > 0$$

$$T = T_0 \quad \text{at } r = R_0, z > 0$$

$$T = T_\infty \quad \text{at } r = \infty$$

$$x_A = x_{A0} \quad \text{at } r = R_0, z > 0$$

$$x_A = x_{A\infty} \quad \text{at } r = \infty$$

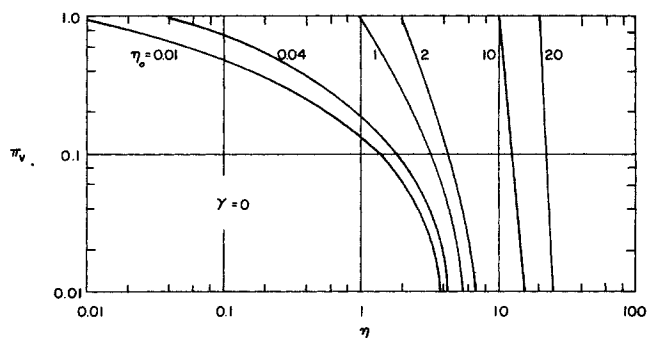


Fig. 2. Π_v vs. η for the case $\gamma = 0$.

It will be assumed that species A diffuses into a medium which will be binary in A and B and that, at $r = R_0$, the flux of B vanishes, so that

$$N_B = 0 \quad \text{at } r = R_0$$

The flux N_A is related to the velocity v_{r0} by

$$v_{r0} = N_{A0}/c_{A0} \quad (5)$$

If the continuity equation is integrated with respect to r , it follows that

$$v_r = \frac{R_0 v_{r0}}{r} - \frac{1}{r} \int_{R_0}^r r \frac{\partial v_z}{\partial z} dr \quad (6)$$

For the case at hand, Fick's law gives

$$N_{A0} = - \frac{c D_{AB}}{(1 - x_{A0})} \frac{\partial x_A}{\partial r} \bigg|_{r=R_0} \quad (7)$$

The radial velocity may then be written as

$$v_r = - \frac{c D_{AB} R_0}{(1 - x_{A0}) c_{A0} r} \frac{\partial x_A}{\partial r} \bigg|_{r=R_0} - \frac{1}{r} \int_{R_0}^r r \frac{\partial v_z}{\partial z} dr \quad (8)$$

The following dimensionless variables and parameters are introduced:

$$\Pi_v = v_z/V \quad (9a)$$

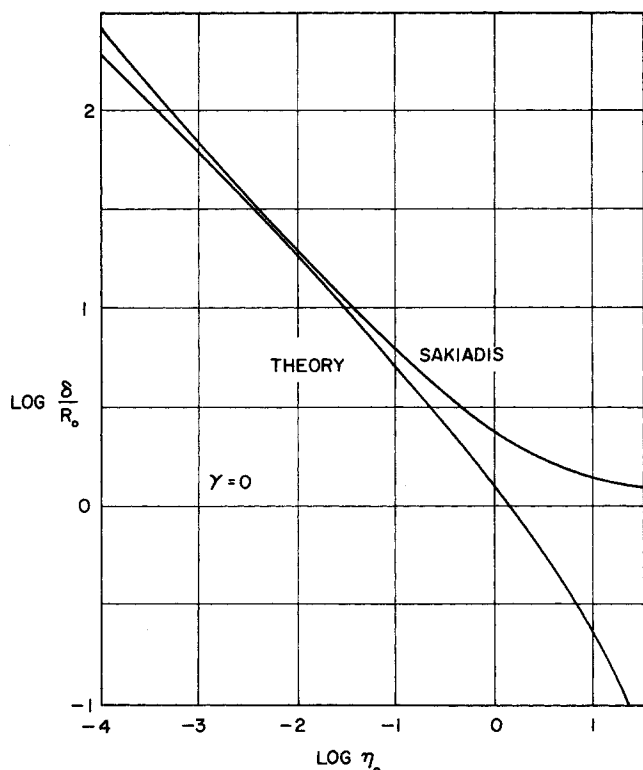


Fig. 3. Reduced boundary-layer thickness δ/R_0 vs. η_0 . δ is defined as the radial distance from the surface to the position at which $\Pi_v = 0.01$.

$$\Pi_T = (T - T_0)/(T_\infty - T_0) \quad (9b)$$

$$\Pi_{AB} = (x_A - x_{A0})/(x_{A\infty} - x_{A0}) \quad (9c)$$

$$\Delta_v = 1 \quad (10a)$$

$$\Delta_T = \nu/\alpha = N_{Pr} \quad (10b)$$

$$\Delta_{AB} = \nu/\mathcal{D}_{AB} = N_{Sc} \quad (10c)$$

Equations (1), (3), and (4) may be represented by a single equation of the form

$$-\left[\frac{c\mathcal{D}_{AB}R_0}{(1-x_{A0})c_{A0}r} \frac{\partial x_A}{\partial r} \right]_{r=R_0} + \frac{1}{r} \int_{R_0}^r r \frac{\partial v_z}{\partial z} dr \quad (11)$$

$$\frac{\partial \Pi_i}{\partial r} + v_z \frac{\partial \Pi_i}{\partial z} = \frac{\nu}{\Delta_i r} \frac{\partial}{\partial r} \left(r \frac{\partial \Pi_i}{\partial r} \right)$$

where Π_i is one of the variables in Equations (9), and Δ_i is the corresponding parameter from Equations (10). The boundary conditions for Equation (11) become

$$\Pi_v = 0 \quad @ \quad r = \infty$$

$$\Pi_T = \Pi_{AB} = 1$$

$$\Pi_v = 1$$

$$@ \quad r = R_0$$

$$\Pi_T = \Pi_{AB} = 0$$

It can be verified that a similarity transformation of the form

$$\eta = \frac{V}{4\nu} \frac{r^2}{z} \quad (12)$$

reduces Equation (11) to an ordinary differential equation

$$\frac{d^2 \Pi_i}{d\eta^2} + \frac{\Delta_i}{\eta} f \frac{d\Pi_i}{d\eta} = 0 \quad (13)$$

with boundary conditions

$$\Pi_v = 0$$

$$@ \quad \eta = \infty$$

$$\Pi_T = \Pi_{AB} = 1$$

$$\Pi_v = 1$$

$$@ \quad \eta = \eta_0 = \frac{VR_0^2}{4\nu z}$$

$$\Pi_T = \Pi_{AB} = 0$$

In Equation (13), a function f appears which is given by

$$f = -\gamma + \eta_0 + \frac{1}{\Delta_i} + \int_{\eta_0}^{\eta} \Pi_v d\eta \quad (14)$$

A dimensionless mass flux γ is defined as

$$\gamma = \frac{c(x_{A0} - x_{A\infty})}{\Delta_{AB}c_{A0}(1 - x_{A0})} \eta_0 \frac{d\Pi_{AB}}{d\eta} \bigg|_{\eta=\eta_0} \quad (15)$$

Equation (13) may be integrated to give Π_v as

$$\Pi_v = 1 - \int_{\eta_0}^{\eta} \exp\left(-\int_{\eta_0}^{\eta''} \frac{f}{\eta'} d\eta'\right) d\eta'' \bigg/ \int_{\eta_0}^{\infty} \exp\left(-\int_{\eta_0}^{\eta''} \frac{f}{\eta'} d\eta'\right) d\eta'' \quad (16)$$

Since f depends upon Π_v and Π_{AB} , Equation (16) is an implicit solution for Π_v . Solutions for Π_T and Π_{AB} may be written as

$$\Pi_{AB} = \int_{\eta_0}^{\eta} \exp\left(-\int_{\eta_0}^{\eta''} \frac{\Delta_{AB}f}{\eta'} d\eta'\right) d\eta'' \bigg/ \int_{\eta_0}^{\infty} \exp\left(-\int_{\eta_0}^{\eta''} \frac{\Delta_{AB}f}{\eta'} d\eta'\right) d\eta'' \quad (17)$$

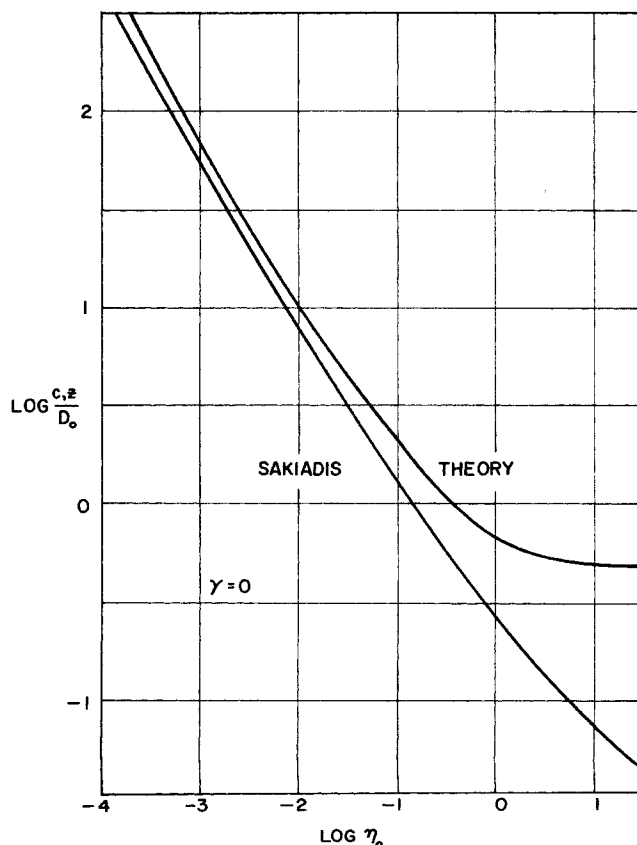


Fig. 4. Local friction coefficient c_f for the case $\gamma = 0$.

with an identical equation (except for subscripting Π and Λ) for Π_T .

From the Π profiles, the fluxes may be obtained, and these will be presented in terms of a friction coefficient

$$c_f = \frac{\tau_{rz}}{\frac{1}{2} \rho V^2} = -2 \frac{\mu \left(\frac{\partial v_r}{\partial z} + \frac{\partial v_z}{\partial r} \right)}{\rho V^2} \quad (18)$$

Nusselt number

$$N_{Nu} = \frac{q_r D_0}{(T_0 - T_\infty)k} = - \frac{D_0 \frac{\partial T}{\partial r} \Big|_{r=R_0}}{T_0 - T_\infty} \quad (19)$$

and a Sherwood number

$$N_{Sh} = \frac{J_{Ar}^* D_0}{c \mathcal{D}_{AB} (x_{A0} - x_{A\infty})} = - \frac{D_0 \frac{\partial x_A}{\partial r} \Big|_{r=R_0}}{x_{A0} - x_{A\infty}} \quad (20)$$

In terms of the reduced variables, these coefficients are found to be

$$c_f = - \frac{1}{2} \frac{D_0}{z} \Pi'_{v0} \quad (21)$$

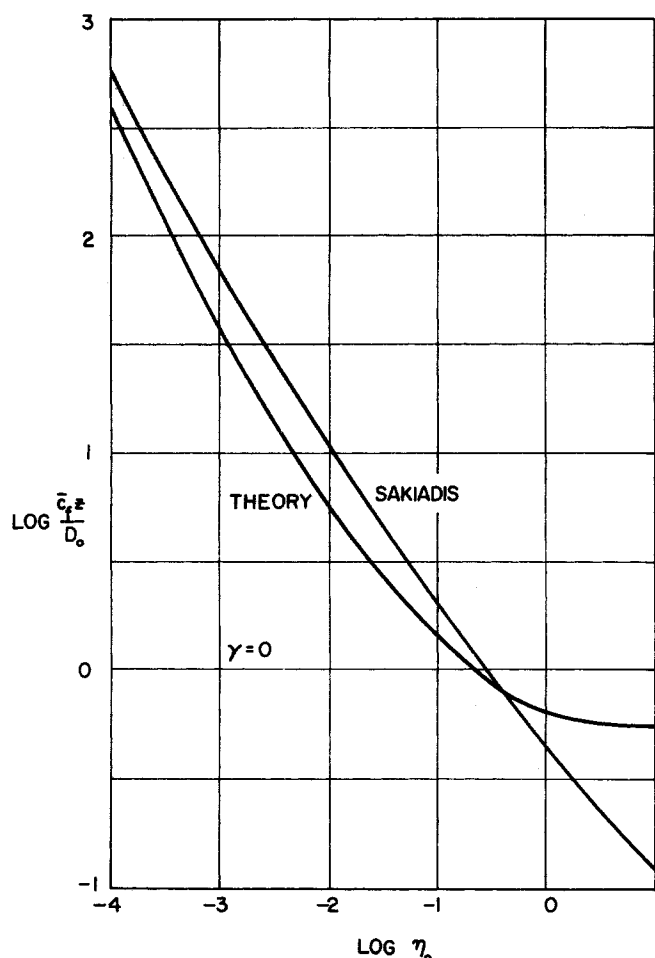


Fig. 5. Integral friction coefficient \bar{c}_f for the case $\gamma = 0$.

$$N_{Nu} = \frac{1}{4} N_{Re} \frac{D_0}{z} \Pi'_{T0} \quad (22)$$

and

$$N_{Sh} = \frac{1}{4} N_{Re} \frac{D_0}{z} \Pi'_{AB0} \quad (23)$$

A jet Reynolds number $N_{Re} = (VD_0)/(\nu)$ has been introduced, and Π'_{i0} is $(d\Pi_i/d\eta)_{\eta=\eta_0}$. The gradients at the jet surface are given by

$$\Pi'_{i0} = \left[\int_{\eta_0}^{\infty} \exp \left(- \int_{\eta_0}^{\eta''} \frac{\Lambda_i f}{\eta'} d\eta' \right) d\eta'' \right]^{-1} \quad (24)$$

where the appropriate Λ_i must be introduced for each Π'_i .

METHOD OF SOLUTION

The solutions have the functional form

$$\Pi_i = \Pi_i(\eta; \eta_0, \gamma, \Lambda_i)$$

and the general procedure for solution is as follows:

1. Values of η_0 , γ , and the Λ_i are assumed.
2. A velocity profile $\Pi_v(\eta)$ is assumed, and f is calculated from Equation (14).
3. A new velocity profile $\Pi_v(\eta)$ is calculated from Equation (16).
4. The two $\Pi_v(\eta)$ profiles are compared and if they differ according to some established criterion, a new f is calculated from Equation (14), and the process repeated until satisfactory convergence of $\Pi_v(\eta)$.
5. With $\Pi_v(\eta)$ and the corresponding f , and the initial choice for γ , Equation (17) is used to calculate Π_{AB} and

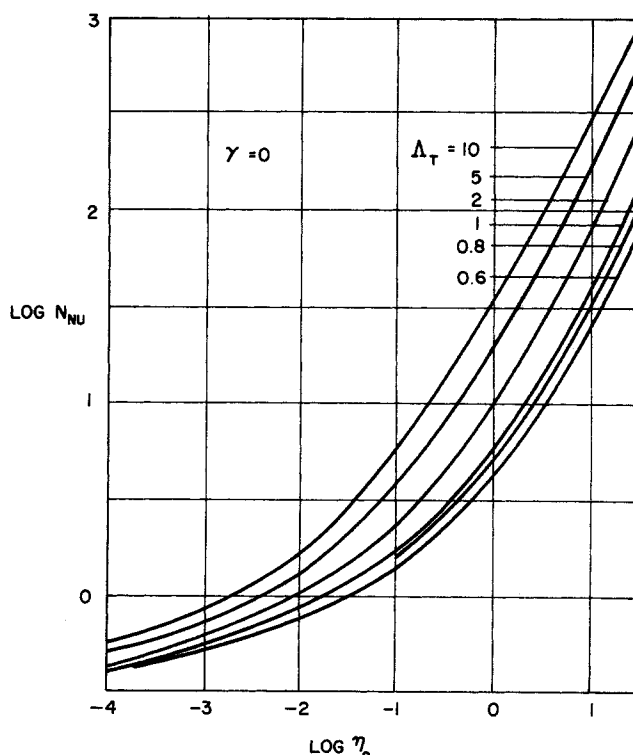


Fig. 6. Local Nusselt numbers for the case $\gamma = 0$.

SOLUTIONS FOR $\gamma = 0$ (NO EFFECT OF MASS TRANSFER)

Figure 2 shows velocity profiles as $\Pi_v(\eta; \eta_0)$. Of major interest is the boundary-layer thickness δ and the friction coefficient c_f . These are shown in Figures 3 and 4, along with the corresponding results of Sakiadis (7). The solutions differ significantly at large η_0 , corresponding to small z . Sakiadis points out that his integral method, based on an assumed form for the velocity profile which does not behave properly at small z , will lead to error in that region.

In fiber spinning calculations, one is interested in the total drag force exerted on the fiber over some length L . This may be calculated from an integral skin friction coefficient \bar{c}_f defined by

$$\bar{c}_f = \frac{1}{L} \int_0^L c_f dz \quad (25)$$

Figure 5 shows \bar{c}_f from the present theory compared with \bar{c}_f from Sakiadis' theory. The region of fiber spinning operation corresponds to η_0 values in the range 10^{-4} to 10^{-2} . Hence, the theory of Sakiadis is indeed accurate for such application.

Experimental studies by Griffith (4) and Koldenhof (5) both confirm the accuracy of Sakiadis' solution in the fiber spinning region. Jet stability studies, on the other hand, cover a range of η_0 of 10^{-4} to 1 (3). In this region, the

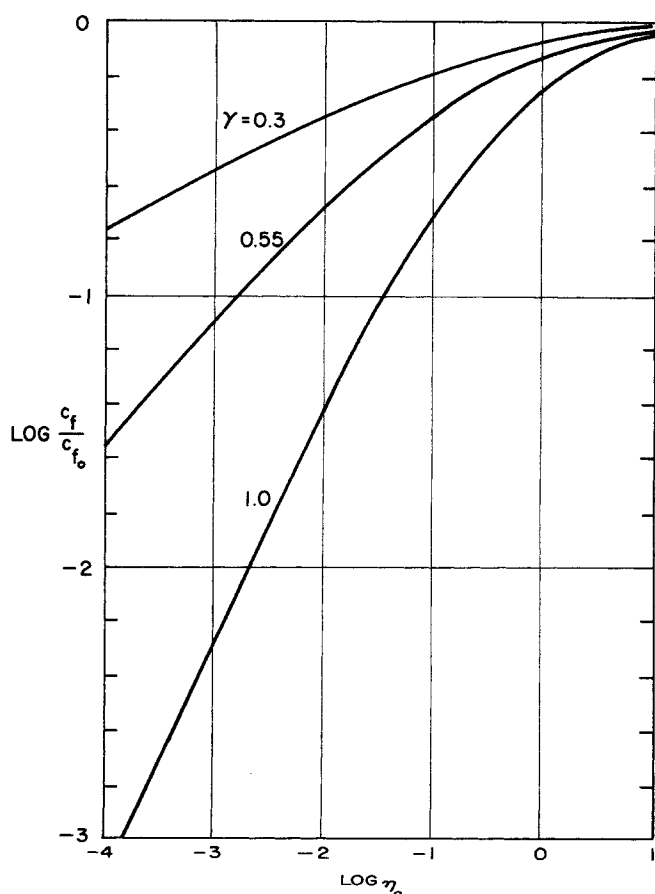


Fig. 7. Reduction in local skin friction due to mass transfer. c_{f0} is c_f for $\gamma = 0$.

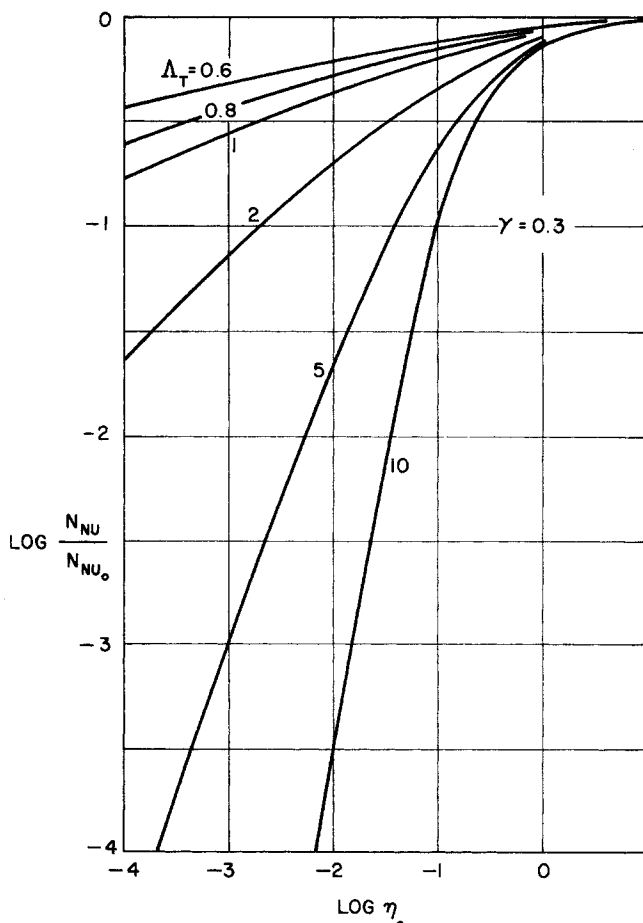


Fig. 8. Reduction in local Nusselt number due to mass transfer, for $\gamma = 0.3$.

theory of Sakiadis begins to deviate markedly from the more exact theory.

Figure 6 shows the local Nusselt number for various values of $\Lambda_T = N_{Pr}$. (The Sherwood number plot is identical, with Λ_T replaced by $\Lambda_{AB} = N_{Sc}$.)

SOLUTIONS FOR $\gamma > 0$ (EVAPORATING JET)

Solutions have been carried out for typical values of the mass transfer parameter γ . Of particular interest is the effect of evaporation on the transfer coefficients c_f , N_{Nu} , and N_{Sh} .

Figure 7 shows the reduction in local drag coefficient due to mass transfer out of the jet. Very near the exit (large η_0) the effect of mass transfer is very slight. Farther downstream very significant reductions in drag may be effected. Parallel results are obtained for the reduction in the local Nusselt (or Sherwood) numbers, as shown in Figures 8 and 9 for two values of γ .

For the special (but interesting) case in which $x_{A0} = 0$, Equation (15) for γ reduces to

$$\gamma = \frac{1}{\Lambda_{AB}(1 - x_{A0})} \eta_0 \Pi'_{AB0} \quad (26)$$

The gradient Π'_{AB0} is a function of η_0 and γ . Hence, one may view Equation (26) as an implicit relationship between γ and η_0 , with $\Lambda_{AB}(1 - x_{A0})$ as a parameter. From the theoretical results, one may then solve for $\gamma(\eta_0)$ for various values of $\Lambda_{AB}(1 - x_{A0})$. Figure 10 shows the results.

Having completed such a theoretical analysis, one may

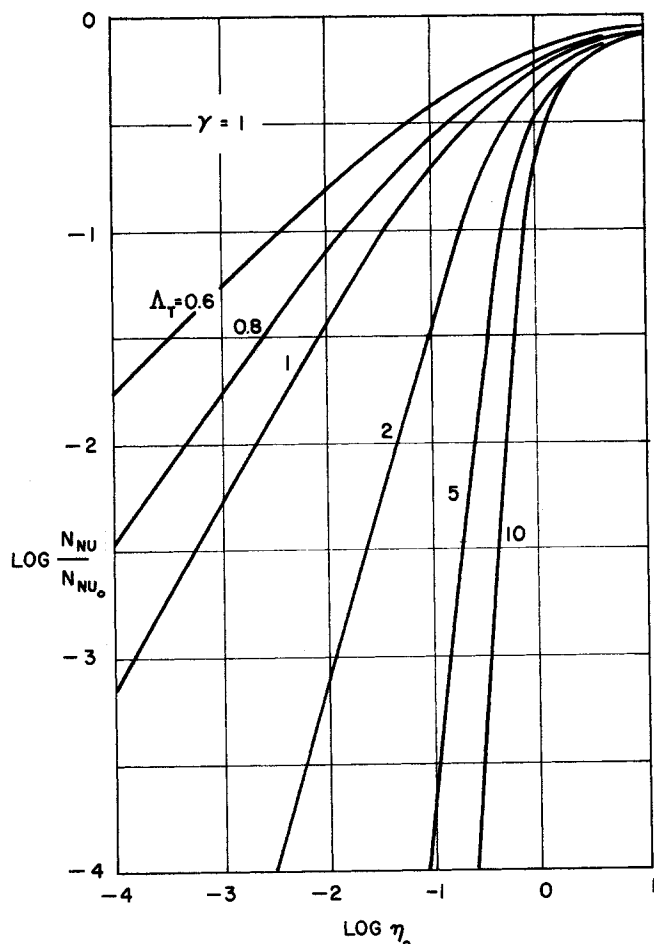


Fig. 9. Reduction in local Nusselt number due to mass transfer, for $\gamma = 1.0$.

return to one of the problems that motivated the theory and ask the question can we expect evaporation to play a significant role in the disruption of a liquid jet? Consider, as an example, a jet of isopropyl alcohol injected into air at atmospheric pressure. The temperature will be taken as 25°C.

From Fenn's data (3), an estimate of η_0 at the point of disruption of the jet, under typical experimental conditions, is $\eta_0 = 0.057$. The vapor pressure of isopropyl alcohol at 25°C. is 44 mm. Hg (8), so x_{A0} may be taken as $44/760 = 0.058$. For Λ_{AB} , the value 0.7 will be used (6). From Figures 10 and 7, one may prepare a tabulation of c_f/c_{f0} at various distances between the jet exit and the breakup point:

η_0 :	0.057	0.114	0.228	0.57
γ :	0.30	0.38	0.51	0.80
c_f/c_{f0} :	0.60	0.60	0.60	0.56

Between the breakup point ($\eta_0 = 0.057$) and a point one tenth of that distance from the exit ($\eta_0 = 0.57$), the local drag coefficient is seen to be substantially reduced by vaporization. Fenn's studies have indicated that the drag exerted by the ambient medium controls the stability of the jet in the neighborhood of the maximum in the breakup curve. Hence, one might expect to find a measurable increase in the stability of the jet in that region. Experiments are in progress to evaluate this point quantitatively.

ACKNOWLEDGMENT

This work was supported by the National Science Foundation under Grant GK1037.

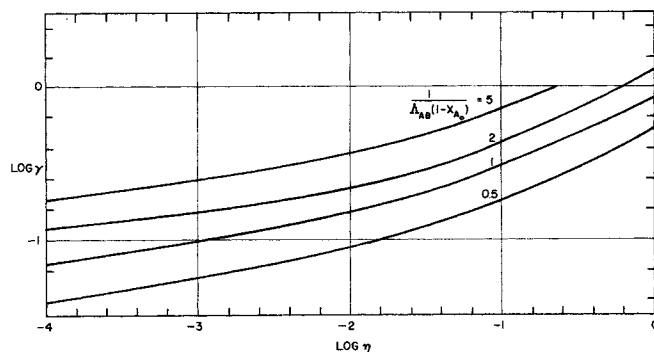


Fig. 10. Mass transfer parameter γ as a function of η_0 .

NOTATION

- c = concentration, moles/cc.
- c_f = local friction coefficient [Equation (18)]
- \bar{c}_f = integral friction coefficient [Equation (25)]
- D = diameter of jet, cm.
- \mathcal{D}_{AB} = diffusivity, sq.cm./sec.
- f = function defined in Equation (14)
- N_A, N_B = molar flux of A or B, moles/(sq.cm.)(sec.)
- N_{Nu} = Nusselt number [Equation (19)]
- N_{Pr} = Prandtl number = ν/α
- N_{Re} = Reynolds number = VD/ν
- N_{Sc} = Schmidt number = ν/\mathcal{D}_{AB}
- N_{Sh} = Sherwood number [Equation (20)]
- r = radial coordinate, cm.
- R_0 = radius of jet, cm.
- T = temperature, °C.
- V = velocity of jet, cm./sec.
- v_r, v_z = radial and axial components of velocity in the ambient medium, cm./sec.
- x_A = mole fraction of component A
- z = axial coordinate, cm.

Greek Letters

- α = thermal diffusivity, sq.cm./sec.
- γ = mass flux parameter [Equation (15)]
- δ = boundary-layer thickness, cm.
- η = similarity transform [Equation (12)]
- ν = kinematic viscosity of ambient medium, sq.cm./sec.
- Λ = defined in Equations (10a), (b), (c)
- Π = defined in Equations (9a), (b), (c)

Subscripts

- 0 = quantities evaluated at $r = R_0$
- ∞ = quantities evaluated at $r = \infty$

LITERATURE CITED

1. Andrews, E. H., *Brit. J. Appl. Phys.*, **10**, 39 (1959).
2. Bird, R. B., W. E. Stewart, and E. N. Lightfoot, "Transport Phenomena," p. 608, Wiley, New York (1960).
3. Fenn, R. W., and Stanley Middleman, *AIChE J.*, **15**, No. 3, 379 (May, 1969).
4. Griffith, R. M., *Ind. Eng. Chem. Fundamentals*, **3**, 245 (1964).
5. Koldenhof, E. A., *AIChE J.*, **9**, 411 (1963).
6. McCabe, W. L., and J. C. Smith, "Unit Operations of Chemical Engineering," p. 926, McGraw-Hill, New York (1956).
7. Sakiadis, B. C., *AIChE J.*, **7**, 467 (1961).
8. Timmermans, J., "Physico-chemical Constants of Pure Organic Compounds," Vol. 1, Elsevier, New York (1950).

Manuscript received October 28, 1968; revision received January 15, 1969; paper accepted January 20, 1969.